Hindawi
International Transactions on Electrical Energy Systems
Volume 2022, Article ID 1152708, 9 pages
https://doi.org/10.1155/2022/1152708

Research Article

Automatic Distributed Control Method for Indoor Low-Voltage Electricity Based on Modal Symmetry Algorithm

Han Lian

School of Electronic Information Engineering, Henan Polytechnic Institute, Nanyang 473009, China

Correspondence should be addressed to Han Lian; lianhan@mjcedu.cn

Received 21 June 2022; Revised 8 September 2022; Accepted 12 September 2022; Published 24 September 2022

Academic Editor: Ali Q. Al-Shetwi

The traditional control method has a low margin of indoor voltage stability, which can easily lead to voltage collapse, and the control effect is not ideal. An automatic distributed control method for indoor low-voltage electricity system based on modal symmetry algorithm is proposed. In order to improve the voltage stability margin, the decoupling between the indoor low-voltage electricity characteristics and regions was analyzed. Based on the analysis results, the decoupling between regions and the robustness to faults of the distributed zone scheme were considered comprehensively, and the modularity and the optimal zoning scheme were screened. Based on the principle of modal symmetry, the original data of the distributed control matrix of low-voltage electricity was obtained. Mean standardization method was used to standardize the matrix, so as to realize the distributed control of indoor low-voltage electricity. The experimental results show that the proposed method improves the margin of voltage stability, overcomes the drawbacks of traditional methods, and reduces the probability of voltage accidents. It shows that this method has higher flexibility, higher reliability, and higher application value as well as improving the automatic control level of voltage.

1. Introduction

With the progress and development of science and technology, distributed control system technology has been widely used in electric automation engineering of power plants. Its own characteristics have been generally recognized. Rational application of distributed control system can improve the automation level of power plants and achieve higher flexibility and reliability of electric automation of power plants [1–3]. The integration of distributed control system into indoor environment is helpful to improve the level of voltage automation. Distributed control system is called DCS. In the process of control, a collection station is composed of several microprocessor cores [4–6]. It can organically combine computer technology, communication technology, display technology, and control technology, connects different functions and local computers, and has the advantages of good monitoring performance, high reliability, good expansibility, and easy maintenance [7–9]. With the interconnection of cross-regional power grids and constraints from economy and technology, in order to make the full use of existing system resources, power grids are often forced to operate near the critical point, and the voltage stability margin is very low, which increases the probability of power accidents such as voltage collapse [10–12]. In order to ensure voltage quality and reactive power balance, and realize the optimal coordination between voltage stability and reactive power optimization, the automatic distributed control of indoor low-voltage electricity system has become an important measure [13, 14]. At present, the relevant researchers have studied the low-voltage electricity control method and achieved some research results.

In the field of distributed control of power system, there have been relevant studies based on swarm algorithm, neural network, hybrid system theory, and other methods. Some scholars proposed a nonlinear distributed controller based on the swarm algorithm. The controller receives part of the real-time state information of the power grid through the phasor measurement unit and realizes local information

interaction with the weight matrix. The controllable external energy storage equipment with fast action characteristics is used to control the output (or absorption) active power in the generator bus, so as to realize the transient recovery of the system quickly and efficiently. In reference [15], a distributed adaptive controller based on radial basis function neural network (RBFNN) was proposed. The method based on RBFNN was used to compensate the unknown nonlinear items and external disturbances in the system, and the corresponding adaptive parameter estimation method was designed to approximate the ideal weight matrix of the unknown nonlinear items. For the control of low-voltage power, the relevant research mainly focused on the application of automatic power control system in low-voltage distribution system. The automatic power control system mainly includes digital power measurement and control device, multi-function power instrument, control equipment, bus concentrator, monitoring system and communication module. Automatic power control system can be divided into hierarchical structure and distributed structure. According to the composition of some multi-functional power instruments, serial ports were used to connect them and automatically connect them to the power control system. Bus is used to connect and unify the components. In addition, researchers have designed intelligent low-voltage power capacitors to improve the voltage quality in low-voltage AC power systems. However, the design of power automatic control system and low-voltage power capacitor is not fully constrained. In references [16, 17], a regional generator reactive power reserve method based on voltage control zoning was proposed. This method synthetically measured the reactive power reserve value of static voltage stability and quasi-steady voltage control and the availability of reactive power reserve, and analyzed the characteristics and selection methods of control variables. A quadratic programming model for optimizing regional reactive power reserve and regional voltage level was established. However, this method had a low-voltage stability margin, thereby reducing the voltage level. In reference [18], "all PV nodes in the power grid should be relaxed to PQ nodes" was proposed, and the voltage over limit nodes could be calculated by the power flow equation in the form of injected current. The linear sensitivity between the voltage over limit node and the voltages of other nodes in the power grid could be continuously adjusted until the voltage over limit of the entire network node was no longer exceeded. The number of center points of the whole network was determined as the number of partitions to be divided, and the linear sensitivity between the node voltage and the reactive current injected into the node was taken as the scale of the reactive voltage. The reactive power control space was established. However, due to the complexity of the process, the voltage stability margin decreased. In reference [19], an electromagnetic loop network division and scheme evaluation method based on the improved GN splitting algorithm was proposed. According to the importance of the shrinking nodes, the feature node integrator was selected, and then, the edge median was obtained using the GN splitting algorithm to evaluate the weakness of the straight line, so as to obtain the segmentation scheme. An information entropy evaluation model based on two-level indicators was constructed to evaluate the ring network division scheme. Although this method was effective, it did not control the indoor voltage and lack pertinence [20, 21].

In order to solve the problems of the traditional methods mentioned above, improve the voltage stability margin and fully constrain the control conditions, an automatic distributed control method for indoor low-voltage electricity system based on modal symmetry algorithm was proposed. Experiments show that this method effectively solved the problem of low-voltage stability margin that easily to lead to voltage collapse accident and improved the control effect [22, 23].

2. Automatic Distributed Control Method for Indoor Low-Voltage Electricity

2.1. Characteristics of Low-Voltage Electricity. Low-voltage electrical apparatus is an electrical apparatus that plays the role of protection, control, regulation, conversion, and on-off in the circuit with rated voltage of AC 1000 V or DC 1500 V. The power range is generally 100 W to 1000 W. The rated voltage of low-voltage appliances shall be compatible with the nominal voltage of the circuit, and the rated impulse withstand voltage shall be compatible with the overvoltage category required by the installation site. The rated frequency of low-voltage apparatus shall conform to the nominal frequency of the circuit and the rated current shall not be less than the load calculation current of the circuit. Indoor low-voltage distribution devices are mainly composed of switching appliances and control appliances. They are mainly used for power conversion, shunting, and regulation of electrical equipment. Once an accident occurs, the accident electrical appliances can be cut off in time without affecting the normal work of non-accident electrical appliances. Therefore, the automatic distributed control of indoor low-voltage electrical appliances is conducive to reducing the probability of accidents and ensuring personal safety. Distributed control of indoor low-voltage electricity system is the decoupling of regional voltage control and the improvement of voltage stability margin. According to the current research, the distributed areas should follow the following principles.

(1) Representation of the central node: the voltage characteristics of the central node in the region can reflect the voltage characteristics of all the nodes in the region.

(2) Controllability in the area: there is enough reactive power reserve in the area to control the voltage in the area.

(3) Inter-regional decoupling: the regional voltage is controlled by the reactive power source in the region and is less affected by other regions.

(4) Robustness to faults: before and after faults, the changes of electrical connections between nodes should be small; otherwise, the zoning scheme may

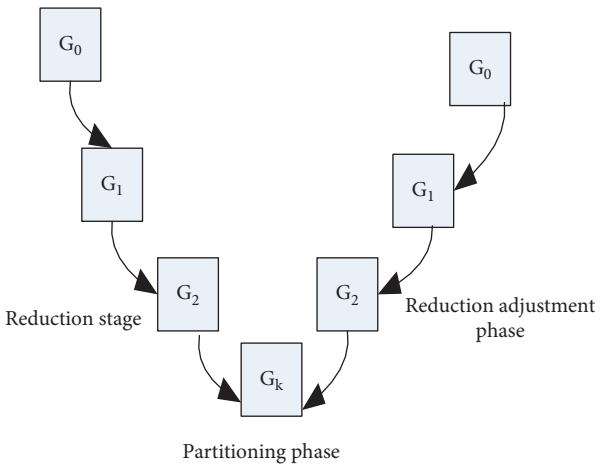

Figure 1: Transformer branch network.

lose reference value, and the control optimization measures in the region may also fail. This principle can be regarded as an extension of the concept of inter-regional decoupling.

(5) Connectivity within a region: there are no isolated nodes within the region or separated by other regions.

(6) Consistency of transformer's branch endpoint: transformer's branch node belongs to the same area.

According to the given transformer network structure and regional operation conditions, the node method was used to make power flow calculation, and the operation state of indoor low-voltage power network was obtained. Taking the symmetry matrix of indoor low-voltage power automatic distributed control as the objective function, the voltage and reactive power of nodes will be constrained. In the above principles, the central node can be determined after the scheme of distributed area was obtained. Principles (5) and (6) will be guaranteed in the algorithm, so the process should focus on meeting principles (2)–(4). The following is a detailed analysis of the controllability and decoupling between regions. Figure 1 shows the branch network of the transformer.

2.1.1. Controllability Analysis of Indoor Area: Electrical Distance of Reactive Power Node. The ability of reactive power source (such as generator and SVC) nodes to control the voltage of controlled nodes can be characterized by quasi-steady-state voltage control sensitivity.

$$\Delta U_L = \frac{\partial U_L}{\partial Q_G}\Delta Q_G = S_{LG}\Delta Q_G, \tag{1}$$

where ΔQ_G is the variation vector of reactive power output of indoor low-voltage electricity distributed control, ΔU_L is the voltage variation vector of controlled node of low-voltage electricity distributed control, G is the reactive power node set, L is the controlled node set (including reactive power node whose reactive power output has reached the upper limit), and S_{LG} is the sensitivity matrix of low-voltage

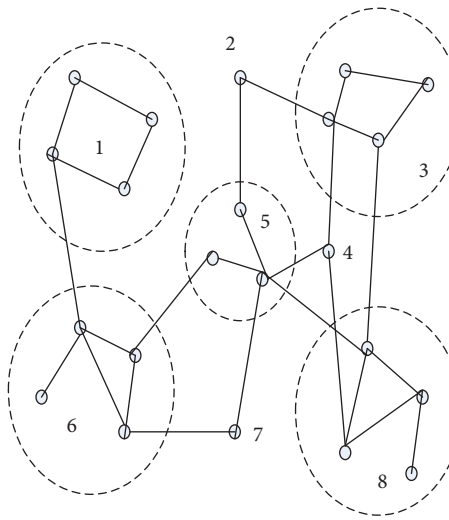

Figure 2: Topology of the power grid.

electricity distributed control. Element $(S_{LG})_{ij}$ represents the voltage variation of the controlled node i when the unit of reactive power output of reactive power source j changes. In order to meet the quasi-steady-state distributed control characteristics of low-voltage electricity system, the successive recursive method is used to solve the problem, that is, when calculating the control sensitivity of a reactive power node, the remaining reactive power nodes are still set as PV nodes [24].

S^i_{LG} is the low-voltage electricity distributed control vector of each reactive power node to the controlled node. Because of the regional characteristics of distributed control of low-voltage electricity system, in S^i_{LG}, the corresponding components of the controlled nodes near the reactive power node i are larger, while the other components are smaller. If the voltage control vectors of reactive power node i and j are similar, it shows that their reactive power reserve can be used to control the voltage level in their vicinity, and the control coupling degree is high. Therefore, the electrical distance of reactive power node can be defined as

$$D\left(S^i_{LG}, S^j_{LG}\right) = 1 - \frac{\left(S^i_{LG}\right)^T S^j_{LG}}{\left\|S^i_{LG}\right\|\left\|S^j_{LG}\right\|}. \tag{2}$$

According to formula (2), the electrical distances of partitions s and t are defined.

$$D\left(G_s, G_t\right) = \max\left(D\left(S^i_{LG}, S^j_{LG}\right)\right), \tag{3}$$

where G_s and G_t are reactive power node sets in distributed area s and t, respectively. If the electrical distances of s and t in the distributed area are similar, it shows that the control function of reactive power sources in the distributed area s and t is similar, and priority should be given to merging in the distributed process to meet the principle of controllability in the area. Figure 2 shows the network topology.

2.1.2. Interregional Decoupling Analysis: Modularity and Optimal Scheme Screening. In the process of decentralization, a series of partitioning schemes are generated, among

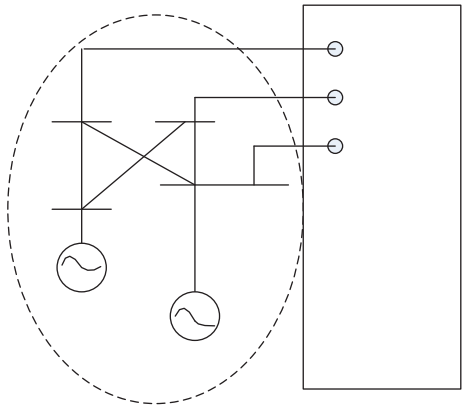

Figure 3: A simplified cluster of nodes with reactive power source nodes.

which the most reasonable one with decoupling property should be chosen as the optimal one. An index for evaluating the quality of partition is proposed. The weighted definition is as follows:

$$M\left(A,\Phi_p\right)=\frac{1}{2m}\sum_i\sum_j\left(A_{ij}-\frac{k_ik_j}{2m}\right)\delta(i,j), \tag{4}$$

where A is the edge weight matrix, element A_{ij} is the edge weight of connecting nodes i and j; Φ_p is the distributed zone scheme; if node i and j belong to the same partition, then $\delta(i,j)=1$, otherwise $\delta(i,j)=1$; $k_i=\sum_i A_{ij}$ is the sum of all edge weights connected with node i, i.e., the degree of node i; $m=1/2\sum_i\sum_j A_{ij}$ is the sum of all edge weights in the network; $k_ik_j/2m$ is the expected value of edge weights between nodes i and j in the case of random network connection to keep the degree of nodes i and j unchanged. By analyzing of formula (4), if the value of M is to be increased, it is necessary to divide the nodes at both ends of the branch whose weight is greater than the expected value (i.e., the connection is close) into the same area, and the nodes at both ends of the branch whose weight is less than the expected value (i.e., the connection is weak) into different areas. Obviously, this is a reasonable way of dividing. Therefore, M can be used to evaluate the quality of zoning. Practical experience shows that when $M>0.3$, the division quality is higher [25, 26]. Figure 3 shows a simplified cluster of nodes with reactive power sources.

In this paper, the power grid is regarded as a weighted undirected connected graph. Nodes and branches are nodes and edges of the graph, respectively. Two modularity indices are proposed to measure the inter-regional decoupling and robustness to faults of the partition scheme.

(1) Interregional Decoupling Modularity M_1. According to the principle of inter-regional decoupling, a reasonable scheme of distributed zone should make the electrical connection of the nodes at both ends of the branch within the region close, and the electrical connection of the nodes at both ends of the branch at the regional boundary weak [27, 28]. In order to reflect the different characteristics of PV node and PQ node, the definition of electrical distance is improved and M_1 is defined.

$$\begin{aligned}
\alpha_{ij}&=\begin{cases}\dfrac{\Delta U_i}{\Delta U_j}=\dfrac{\partial U_i/\partial Q_j}{\partial U_i/\partial Q_j}\,i\in L,\\[2ex] \dfrac{\Delta Q_i}{\Delta Q_j}=\dfrac{\partial Q_i/\partial Q_j}{\partial Q_i/\partial Q_j}\,i\in G,\end{cases}\\
d_{ij}&=d_{ji}=-\ln\left(\alpha_{ij}\alpha_{ji}\right),\\
(A_1)_{ij}&=\begin{cases}\dfrac{1-d_{ij}}{\max\left(d_{ij}\right)}, & y_{ij}\neq 0,\\[2ex] 0, & y_{ij}=0,\end{cases}\\
M_1\left(\Phi_p\right)&=M\left(A_1,\Phi_p\right),
\end{aligned} \tag{5}$$

where U_i and Q_i are the voltage of node i and injection reactive power, respectively; d_{ij} is the electrical connection degree of node i and j; y_{ij} is the admittance value between node i and j. If i is a controlled node, α_{ij} is defined as the voltage change of node i when node j's voltage unit changes; if i is a reactive power node, its voltage does not change; α_{ij} is defined as the variation of node i's reactive power output when node j's reactive power unit changes. The closer the electrical connection between nodes i and j is, the larger the value of α_{ij} is, the smaller the value of d_{ij} and the larger the value of $(A_1)_{ij}$. From the analysis of formula (4), it can be concluded that M_1 can measure the inter-regional decoupling of the distributed zone scheme.

(2) Fault Robustness Modularity M_2. According to the principle of robustness of the distributed zone scheme to faults, if the electrical connection of the nodes at both ends of the branch is greatly weakened due to the fault of the branch, the branch should be regarded as the regional boundary branch. Because it takes more time to calculate the change of electrical connection before and after branch failure one by one, and the divergence of power flow may occur, the sensitivity of the electrical connection of the two ends of the branch to the admittance of the branch is used to characterize the change of electrical connection at the end of the branch before and after the branch break, and the modularity M_2 is defined.

$$\begin{aligned}
\Delta d_{ij}&=\frac{\partial d_{ij}}{\partial y_{ij}}\Delta d_{ij},\\
(A_2)_{ij}&=\begin{cases}\dfrac{1-\Delta d_{ij}}{\max\left(\Delta d_{ij}\right)}, & y_{ij}\neq 0,\\[2ex] 0, & y_{ij}=0,\end{cases}\\
M_2\left(\Phi_p\right)&=M\left(A_2,\Phi_p\right).
\end{aligned} \tag{6}$$

The partial derivative in formula (6) can be calculated by numerical perturbation method. Formula (6) shows that the stronger the robustness of the branch is, the smaller the d_{ij}

value is and the larger the $(A_2)_{ij}$ value is. M_2 can be used to measure the robustness of low-voltage distributed control scheme to faults.

The scheme quality of distributed zone is characterized by M_1 and M_2. The modularity index M_Σ of distributed control is defined.

$$M_\Sigma\left(\Phi_{pi}\right) = \frac{M_1\left(\Phi_{pi}\right)}{\max\left(M_1\left(\Phi_{pi}\right)\right)} + \frac{M_2\left(\Phi_{pi}\right)}{\max\left(M_2\left(\Phi_{pi}\right)\right)}, \quad (7)$$

where Φ_{pi} is the ith partition scheme.

M_Σ takes into account the inter-area decoupling and robustness to faults of the distributed control scheme for indoor low-voltage electricity systems. The scheme corresponding to M_Σ maximum is chosen as the optimal distributed control scheme.

2.2. Automatic Distributed Control Method for Indoor Low-Voltage Electricity Based on Modal Symmetry Algorithm. Based on the optimal distributed area control scheme obtained in Section 2.1, the distributed control matrix of indoor low-voltage electricity system was obtained by using the principle of modal symmetry. Prior to this, the original data need to be prepared, that is, the process of determining the classified objects and extracting the characteristics of each object. The asymmetric modal information of the whole indoor low-voltage electrical device can be obtained by subtracting the average value of the low-voltage electricity linearity collected by two centrosymmetric sensors, thus the asymmetric modal can be extracted from the symmetric modal. Because the asymmetric modal amplitude of some partitions was high, by observing whether the asymmetric modal amplitude of the eigenvector of distributed control for indoor low-voltage electricity had a sudden change, the automatic partition of indoor low-voltage electricity can be accurately processed, which provides conditions for the final distributed control [29].

The universe $U = \{x_1, x_2, \ldots, x_n\}$ is the classified object, where each object is represented by m data that can represent the characteristics of the object, i.e.,

$$x_i = \{x_{i1}, x_{i2}, \ldots, x_{im}\}, \ (i = 1, 2, \ldots n). \quad (8)$$

This forms a raw data matrix R of $m \times n$.

The similarity matrix obtained from the previous step is only reflexive and transitive, and does not have symmetry. It needs to be transformed into equivalent matrix by calculating symmetry coefficient. The concrete method is to start from R and find the square in turn: $R \longrightarrow R^2 \longrightarrow R^4 \longrightarrow \cdots$. When $R^k \cdot R^k = R^k$ appeared for the first time, it shows that R^k has symmetry, and R^k is the symmetry coefficient $t(R)$. Different cut-off values λ were taken and R^k was intercepted to get the required classification. For any $\lambda \in [0, 1]$, $[t(R)]_\lambda = (r_{ij}^\lambda)$ is the λ truncated matrix of $t(R)$, where

$$r_{ij}^\lambda = \begin{cases} 1, & r_{ij} > \lambda, \\ 0, & r_{ij} > \lambda, \end{cases} \quad (9)$$

when $r_{ij}^\lambda = 1$, node i and node j were grouped together. With the change of λ from big to small, classification from fine to coarse is a dynamic process.

The eigenvectors of distributed control for indoor low-voltage electricity describing PQ nodes were determined. Considering the actual process of reactive power and voltage control, the control capability of each generator to the load bus was taken as the eigenvectors of low-voltage electricity distributed control, i.e., $x_i = \{x_{i1}, x_{i1}, \ldots, x_{i\times(k+1)}\}$. The element x_{ij} in x_i represents the sensitivity of generator j to load node i. The specific solutions are as follows:

The iterative equation of reactive power flow based on P-Q decomposition method is

$$-L\Delta V = \Delta Q. \quad (10)$$

The ΔV and ΔQ in this equation correspond to the load bus (PQ node). If the generator bus (PV node) is added to the above modified equation, and the load bus and generator bus are represented by the subscripts D and G, respectively, there are

$$-\begin{bmatrix} L_{DD} & L_{DG} \\ L_{GD} & L_{GG} \end{bmatrix}\begin{bmatrix} \Delta V_D \\ \Delta V_G \end{bmatrix} = \begin{bmatrix} \Delta Q_D \\ \Delta Q_G \end{bmatrix}, \quad (11)$$

where L_{DD} is admittance matrix B'' which does not include the corresponding rows and columns of balanced nodes and PV nodes. L_{DG} and L_{GD} are mutual admittance between generators and load buses, and L_{GG} is self-admittance of generators. The relationship between ΔV and ΔQ is derived from formula (9):

$$\begin{bmatrix} \Delta V_D \\ \Delta V_G \end{bmatrix} = -\begin{bmatrix} L_{DD} & L_{DG} \\ L_{GD} & L_{GG} \end{bmatrix}^{-1}\begin{bmatrix} \Delta Q_D \\ \Delta Q_G \end{bmatrix}. \quad (12)$$

Let

$$\begin{bmatrix} X_{DD} & X_{DG} \\ X_{GD} & X_{GG} \end{bmatrix} = -\begin{bmatrix} L_{DD} & L_{DG} \\ L_{GD} & L_{GG} \end{bmatrix}^{-1}. \quad (13)$$

When the generators' reactive power output changes under the distributed control of indoor low-voltage electricity, assuming that the reactive power of load buses remains unchanged, i.e., $\Delta Q_D = 0$, there are

$$\Delta V_D = X_{DG}\Delta Q_G. \quad (14)$$

X_{DG} is the sensitivity matrix between ΔV_D and ΔQ_G. It has the dimension of impedance. It is a partial sub-matrix related to generator node and load node in the inverse of the augmented B'' matrix. In the previous calculation, X_{DG} is calculated in one time, without considering the quasi-steady-state physical response process of PV nodes. By using the proposed method of constructing reactive power control space, the generator was solved step by step. In the $(m + k + 1)$ node system, it is assumed that all $(k + 1)$ generator nodes were equipped with AVR, which constitutes a set G; m load buses to be partitioned constitute a set D. When calculating the sensitivity of a generator A to other nodes, A was set as PQ node, and the other generator nodes were set as PV nodes. When calculating the sensitivity, the diagonal

elements corresponding to the PV node in the full-dimensional admittance matrix B including the PV node and the balanced node were increased to ensure that the terminal voltage of the node remains unchanged. After constructing such a full-dimensional admittance matrix, the sensitivity of the generator A to the load nodes in the system was solved by calculating X_{DG} according to formula (13). The sensitivity of other generator nodes to load nodes was calculated by this method in turn. In this way, the original data of distributed control matrix $X_{[(m\times(k+1))]}$ for low-voltage electricity was obtained.

It is noteworthy that, reactive power should include generators, switchable capacitors, and SVC which can provide voltage/reactive power support to the system as required in the distributed control of indoor low-voltage electricity. It can be easily extended to other reactive power sources, only by increasing the corresponding dimension in the reactive power space.

In order to unify the characteristic indexes of different dimensions and quantities, the mean standardization method was used to standardize $X_{[(m\times(k+1))]}$, that is,

$$y_{ij} = \frac{x_{ij}}{\overline{x}_j}, \tag{15}$$

where y_{ij} is the standardized data, and $\overline{x}_j$ is the average of column data. After this treatment, the elements in Y are unified within a common range of data characteristics. If it is calculated directly, it may highlight the role of those characteristic indicators with a very large order of magnitude in classification, reduce or even exclude the role of some smaller characteristic indicators in classification, resulting in inaccurate classification results.

When using modal symmetry algorithm for automatic distributed control of indoor low-voltage electricity, a symmetric matrix was established, and the symmetric matrix R was calculated. The elements in matrix R are as follows:

$$r_{ij} = \exp\left(-c\sum_{k=1}^{m}\left|y_{ik} - y_{jk}\right|\right), \tag{16}$$

where r_{ij} is the similarity or proximity between load node i and load node j, the exp operation on r_{ij} is to calculate $e^{-c\sum_{k=1}^{m}|y_{ik}-y_{jk}|}$, and its range is $0 \le r_{ij} \le 1$; c is a specific positive number, and the value makes r_{ij} distribute in [0,1], $c = 1$.

The transfer closure matrix of load nodes was calculated by matrix programming which describes the degree of symmetry between load nodes. Under the threshold $\lambda \in [0, 1]$, different λ can be selected to obtain different λ horizontal truncation matrices, each representing a clustering. When λ changes from 1 to 0, the number of classifications changes from n to 1, which is a dynamic process.

When the number of partitions is unknown, the number of classes c was gradually increased from a smaller value. In this process, the modal symmetry algorithm was used for each selected c. The algorithm block diagram is shown in Figure 4. Obviously, the objective function J decreases monotonously with the increase of c. In the process of increasing c, there will always be some denser points separated. J will decrease, but the speed of reduction will slow down. Thus, the number of partitions can be roughly determined.

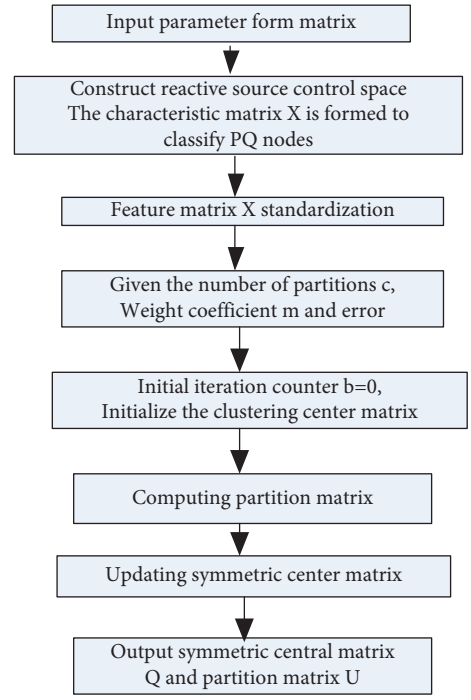

Figure 4: Flow chart of distributed control method for indoor low-voltage electrics.

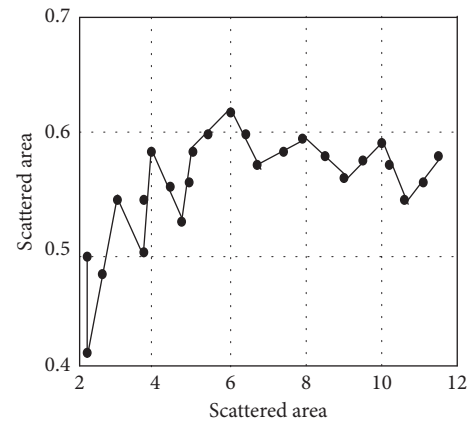

Figure 5: Partition modularity of IEEE 39-node system.

Table 1: Partition results of IEEE39 node system.

Number of distributed area	Node number
1	4, 10, 11, 12, 14, 15, 28
2	1, 2, 4, 16, 24, 26, 30, 35
3	19, 21, 32, 34
4	28, 29, 30
5	16, 22, 24, 26, 36, 37
6	5, 7, 8, 10, 30, 38

Table 2: Comparison of different clustering methods.

Number of tests	Method in reference [17]		Method in reference [18]		Method in reference [19]		The proposed method	
	Modularity	Partition time/s	Modularity	Partition time/s	Modularity	Partition time/s	Modularity	Partition time/s
1	0.4930	1.917	0.5219	1.903	0.5614	1.875	0.6048	1.786
2	0.5568	2.540	0.5677	2.357	0.6076	1.981	0.6408	1.643
3	0.6043	1.835	0.5983	1.833	0.6121	1.764	0.6408	1.738
4	0.6048	2.640	0.6105	2.065	0.6398	1.947	0.6408	1.840
5	0.5743	1.780	0.6059	1.764	0.6316	1.793	0.6408	1.720

Table 3: Verification results of reactive power reserve.

Method of partition	Zone 1	Zone 2	Zone 3	Zone 4	Zone 5	Zone 6
Before partition	33.27	−41.66	24.69	18.16	25.86	74.76
After partition	61.57	80.32	24.69	18.16	25.86	74.76

Table 4: Comparison of modularity of different methods.

Number	Method	Number of distributed zones	Module degree/Q
1	Method in reference [17]	5	0.5643
2	Method in reference [18]	6	0.5701
3	Method in reference [19]	5	0.5755
4	The proposed method	6	0.5991

After selecting the number of partitions and completing the symmetry process of PQ nodes, PV nodes need to be merged. For a PV node connected with only one PQ node, it was merged in the region where the directly connected PQ node was located. Accordingly, the research on automatic distributed control of indoor low-voltage electricity system was completed.

3. Experimental Results and Analysis

The proposed automatic distributed control method for indoor low-voltage electricity system based on modal symmetry algorithm was applied to the standard test system of IEEE-39 nodes and compared with other distributed control methods. The 39-node system consists of 10 generators, 34 lines, and 12 transformers. According to the distributed control method for indoor low-voltage electricity system described above, the maximum number of partitions is 11, that is, the maximum number of iterations of the algorithm is 10. The relationship between modularity M_Σ and number of partitions is shown in Figure 5.

According to the different partition modularity of Figure 5, when the partition number of IEEE39 nodes is 6, the modularity is the highest, and the modularity M_Σ is 0.6049. The results of the preferred partition are shown in Table 1.

Table 2 shows the comparison of modularity and partitioning time of the method in references [17–19] in 6 partition zones. The running environment was Windows 8, and the CPU is i7 quad-core 2.3 GHz. The analysis Table 2 shows that the proposed method has higher stability and shorter partition time than the method in references [17–19]. It can effectively improve the stability margin of the automatic distributed control of indoor low-voltage electricity system.

After checking the optimal zones, it was found that the reactive power reserve index of Zone 2 was 41.67%, which did not meet the requirement of 15% reactive power reserve, and Zone 2 needed to be re-divided. According to the calculation, the feasible dividing nodes in Zone 2 were node 4 (reactive load is 184 Mvar, and the feasible dividing area was Zone 1 and Zone 6) and node 15 (reactive load was 153 Mvar, and the feasible dividing area was Zone 1 and Zone 5). According to the order of reactive load from large to small, the node 4 with larger reactive power was first divided into Zone 1 or Zone 6. If node 4 was divided into Zone 6, the reactive power reserve of Zone 6 will be less than 15%, and Zone 1 of node 4 can ensure the reactive power reserve of all regions. Therefore, node 4 should be divided into partition 1, which effectively improves the margin of low-voltage stability.

The modularity of the six partitions was 0.5992, which was only 0.0057 lower than that of the original partition. Therefore, the new partition had less influence on the inter-regional reactive power coupling and could be used as the final partition scheme. The results of checking and re-partitioning are shown in Table 3.

The proposed method was compared with the methods in references [17], [18], and [19] in terms of partition modularity of the 39-node system. The comparison results are shown in Table 4. It is worth noting that the proposed method is different from other methods, so the modularity values are different, but the results of the same modularity algorithm will not affect the comparison of different partitioning methods.

Table 4 shows that the proposed method has the highest modularity and can effectively improve the margin of voltage stability. The modularity refers to previous M_Σ. At the same time, the proposed method has

some advantages in time complexity and can be used in rapid voltage control zoning after fault or accident in engineering practice.

4. Conclusions

With the development of power network and the emergence of large-scale combined power grid, the problem of voltage stability has become increasingly prominent. Various measures to prevent voltage instability have been proposed, and the voltage hierarchical control system has emerged as the times require. In order to improve the phenomenon of voltage instability and the margin of voltage stability, an automatic distributed control method for indoor low-voltage electricity system based on modal symmetry algorithm is proposed. On the basis of considering the low-voltage electrical characteristics, the principles to be followed in the distribution area were proposed, and the indoor area controllability analysis and inter-area decoupling analysis were made to obtain the optimal distributed area control scheme. The distributed control matrix of indoor low-voltage power system was obtained by using the principle of modal symmetry, and the distributed control of indoor low-voltage power system was completed. The applicability and effectiveness of the designed method were verified through comparative experiments. The experimental results show that the proposed method had the highest module stability and the shortest partition time. It shows that the method in this paper can effectively improve the stability margin of indoor low-voltage power distributed control, which has more advantages than the control method, and can provide valuable reference for low-voltage power system control.

Although this paper has done some useful research and exploration in the field of automatic distributed control of low-voltage electricity system, there are still some problems to be further studied and perfected. When dividing the area, the following criteria are met: strong coupling in the area, weak coupling between the areas; moderate number of voltage control areas; moderate size of each voltage control area; reactive power balance in the area, and a certain amount of reactive power margin left. However, there is a lack of a quantitative criterion to judge the quality of the partition, so the method needs further study.

Data Availability

The datasets used and/or analyzed during the current study are available from the corresponding author on reasonable request.

Conflicts of Interest

It is declared by the authors that this article is free of conflicts of interest.

References

[1] A. Komaee, "Feedback control for transportation of magnetic fluids with minimal dispersion: a first step toward targeted magnetic drug delivery," *IEEE Transactions on Control Systems Technology*, vol. 12, no. 99, pp. 1–16, 2016.

[2] M. Luo and H. Pan, "A numerical study on the relation between the electrical spectra of a mixture and the electrical properties of the components of the mixture," *Journal of Applied Geophysics*, vol. 112, no. 2, pp. 33–41, 2015.

[3] L. Zhang, D. Liu, G. Cai, L. Lyu, L. H. Koh, and T. Wang, "An optimal dispatch model for virtual power plant that incorporates carbon trading and green certificate trading," *International Journal of Electrical Power & Energy Systems*, vol. 144, Article ID 108558, 2023.

[4] A. A. Nikitin, A. B. Ustinov, V. V. Vitko et al., "Dispersion characteristics of spin-electromagnetic waves in planar multiferroic structures," *Journal of Applied Physics*, vol. 118, no. 18, pp. 183901–183952, 2015.

[5] L. Bogataj, M. Vidmar, and B. Batagelj, "Improving the side-mode suppression ratio and reducing the frequency drift in an opto-electronic oscillator with a feedback control loop and additional phase modulation," *Journal of Light-wave Technology*, vol. 34, no. 3, pp. 885–890, 2016.

[6] H. Wang, K. Hou, J. Zhao, X. Yu, H. Jia, and Y. Mu, "Planning-oriented resilience assessment and enhancement of integrated electricity-gas system considering multi-type natural disasters," *Applied Energy*, vol. 315, Article ID 118824, 2022.

[7] C. Lee, T. Kim, H. Park, and S. S. Yang, "Stability improvement of nonthermal atmospheric-pressure plasma jet using electric field dispersion," *Microelectronic Engineering*, vol. 145, no. 9, pp. 153–159, 2015.

[8] Y. Salathiel, Y. Amadou, G. Betchewe, S. Y. Doka, and K. T. Crepin, "Soliton solutions and traveling wave solutions for a discrete electrical lattice with nonlinear dispersion through the generalized riccati equation mapping method," *Nonlinear Dynamics*, vol. 87, no. 4, pp. 2435–2443, 2016.

[9] S. Heslop, I. Macgill, and J. Fletcher, "A practical distributed voltage control method for efficient and equitable intervention of distributed devices," *IET Smart Grid*, vol. 2, no. 3, pp. 399–406, 2019.

[10] B. L. Li, H. L. Zou, L. Lu et al., "Size-dependent optical absorption of layered MoS2 and DNA oligonucleotides induced dispersion behavior for label-free detection of single-nucleotide polymorphism," *Advanced Functional Materials*, vol. 25, no. 23, pp. 3541–3550, 2015.

[11] Z. Jafari and F. Emami, "Simultaneous dispersion flattening for both transverse electric and magnetic modes," *Journal of Lightwave Technology*, vol. 33, no. 1, pp. 212–218, 2015.

[12] X. Xie and D. Chen, "Data-driven dynamic harmonic model for modern household appliances," *Applied Energy*, vol. 312, Article ID 118759, 2022.

[13] Y. Tian, Y. Gong, D. Meng, Y. Li, and B. Kuang, "Dielectric dispersion, diffuse phase transition, and electrical properties of bct-bzt ceramics sintered at a low-temperature," *Journal of Electronic Materials*, vol. 44, no. 8, pp. 2890–2897, 2015.

[14] I. A. Bogachev, I. I. Chernov, M. S. Stal'Tsov et al., "Optimization of electric-pulse consolidation regimes to obtain high-density dispersion-hardened reactor steel," *Atomic Energy*, vol. 120, no. 1, pp. 37–43, 2016.

[15] S. Chen, J. Lu, and Y. Gao, "Distributed adaptive control of power system transient stability based on neural network," *Control and Decision-Making*, vol. 36, no. 6, pp. 1407–1414, 2021.

[16] H. Zhou, C. Xu, C. Lu et al., "Investigation of transient magnetoelectric response of magnetostrictive/piezoelectric composite applicable for lightning current sensing," *Sensors and Actuators A: Physical*, vol. 329, Article ID 112789, 2021.

[17] Y. Song, H. Z. Cheng, J. Zhang, Q. Wang, Q. Sun, and S. Li, "A Generator reactive power reserve optimization method based on voltage control areas," *Automation of Electric Power Systems*, vol. 39, no. 4, pp. 33–39, 2015.

[18] Y. Cheng and N. S. Hang, "Reactive voltage control partitioning based on power network pilot node identification," *Electric Power Automation Equipment*, vol. 35, no. 8, pp. 45–52, 2015.

[19] X. N. Su, T. Q. Liu, B. Wang, H. Jiao, and F. Tang, "A method of electromagnetic loop network partition and schemes assessment based on improved GN split algorithm," *Proceedings of the CSEE*, vol. 37, no. 6, pp. 1686–1694, 2017.

[20] C. Lu, H. Zhou, L. Li et al., "Split-core magnetoelectric current sensor and wireless current measurement application," *Measurement*, vol. 188, Article ID 110527, 2022.

[21] L. Guo, C. Ye, Y. Ding, and P. Wang, "Allocation of centrally switched fault current limiters enabled by 5 g in transmission system," *IEEE Transactions on Power Delivery*, vol. 36, no. 5, pp. 3231–3241, 2021.

[22] Y. Zhang, X. Shi, H. Zhang, Y. Cao, and V. Terzija, "Review on deep learning applications in frequency analysis and control of modern power system," *International Journal of Electrical Power & Energy Systems*, vol. 136, Article ID 107744, 2022.

[23] H. Li, K. Hou, X. Xu, H. Jia, L. Zhu, and Y. Mu, "Probabilistic energy flow calculation for regional integrated energy system considering cross-system failures," *Applied Energy*, vol. 308, Article ID 118326, 2022.

[24] A. Salam, "Dispersion energy shifts among bodies with arbitrary electric multipole polarisability: molecular QED theory," *Molecular Physics*, vol. 113, no. 3-4, pp. 226–231, 2015.

[25] O. H. Nusierat, L. Cremaldi, and I. Ostrovskii, "Acousto-electric admittance of two-dimensional ferroelectric metamaterial under dispersion curve branching," *Journal of the Acoustical Society of America*, vol. 137, no. 4, p. 2299, 2015.

[26] H. Wang, X. Wu, X. Zheng, and X. Yuan, "Virtual voltage vector based model predictive control for a nine-phase open-end winding PMSM with a common DC bus," *IEEE Transactions on Industrial Electronics*, vol. 69, no. 6, pp. 5386–5397, 2022.

[27] M. Medveď, S. Budzak, A. D. Laurent, and D. Jacquemin, "Direct and indirect effects of dispersion interactions on the electric properties of weakly bound complexes," *The Journal of Physical Chemistry A*, vol. 119, no. 12, pp. 3112–3124, 2015.

[28] S. Lu, Y. Ban, X. Zhang et al., "Adaptive control of time delay teleoperation system with uncertain dynamics," *Frontiers in Neurorobotics*, vol. 16, Article ID 928863, 2022.

[29] C. Guo, C. Ye, Y. Ding, and P. Wang, "A multi-state model for transmission system resilience enhancement against short-circuit faults caused by extreme weather events," *IEEE Transactions on Power Delivery*, vol. 36, no. 4, pp. 2374–2385, 2021.